How does breakup influence the total fusion of ^{6,7}Li at the Coulomb barrier?

A. Diaz-Torres*
Institut für Theoretische Physik der Justus-Liebig-Universität Giessen, Heinrich-Buff-Ring 16, D-35392 Giessen, Germany

I. J. Thompson
Physics Department, University of Surrey, Guildford GU2 7XH, United Kingdom

C. Beck
Institut de Recherches Subatomiques, UMR 75000,CNRS-IN2P3 et Université Louis Pasteur, 23 rue du Loess, Boîte Postale 28, F-67037 Strasbourg, Cedex 2, France

(Received 11 June 2003; published 20 October 2003)

Total (complete+incomplete) fusion excitation functions of ^{6,7}Li on ^{59}Co and ^{209}Bi targets around the Coulomb barrier are obtained using a new continuum discretized coupled channel method of calculating fusion. The relative importance of breakup and bound-state structure effects on total fusion is particularly investigated. The effect of breakup on fusion can be observed in the total fusion excitation function. The breakup enhances the total fusion at energies just around the barrier, whereas it hardly affects the total fusion at energies well above the barrier. The difference between the experimental total fusion cross sections for ^{6,7}Li on ^{59}Co is notably caused by breakup, but this is not the case for the ^{209}Bi target.

DOI: 10.1103/PhysRevC.68.044607 PACS number(s): 25.70.Jj, 25.70.Mn, 24.10.Eq

I. INTRODUCTION

The effect of breakup of weakly bound projectiles on fusion has been extensively investigated in recent years both experimentally [1–14] and theoretically [15–22], but there is not yet a definitive conclusion. Experimental works discuss the effect of breakup on fusion by comparing experimental fusion excitation functions to either realistic theoretical predictions which do not include couplings to the breakup channels, e.g., Refs. [5,7,11,13], or to experimental fusion excitation functions of well-bound (reference) projectiles for which the breakup is expected to be weak, e.g., Refs. [4,8,10,12].

In fusion of weakly bound nuclei, two independent fusion processes can be distinguished, namely, complete fusion and incomplete or partial fusion. The total fusion is the sum of these processes (complete + incomplete). These two types of fusion processes are connected to the dynamics of the projectile fragments. A clear definition of complete and incomplete fusion is necessary to compare theoretical predictions to experimental data. Theoreticians, e.g., Refs. [15,16], and experimentalists, e.g., Refs. [5,23], give different definitions in the literature. From a theoretical point of view we think that, strictly speaking, complete fusion refers to the capture of all the projectile fragments (from bound and breakup states) by the target, whereas the incomplete fusion is related to the capture of only some of those fragments. Experimentalists [5,23] tend to define complete and incomplete fusion as absorption of all the charge of the projectile and of a part of that charge, respectively. These definitions are only equivalent to the strictly theoretical ones if all the projectile fragments are charged (e.g., ^{6}Li=α+d or ^{7}Li=α+t), but this is not the case for projectiles such as ^{9}Be=α+α+n or ^{11}Be =^{10}Be+n. It is important to note that in fusion experiments with ^{9}Be [5,10] and ^{11}Be [10] it is still unclear what happens to the valence neutron after the reaction. If we follow the experimental definitions, the total and complete fusion would be the same for the reaction ^{11}Be+^{209}Bi [10], since only the capture of the stable ^{10}Be core has been observed so far.

Most experiments [1–4,6–10,12,14] have only measured the total fusion, whereas in Refs. [5,11,13] the complete fusion was distinguished from the incomplete one. The importance of distinguishing between complete and incomplete fusion in order to observe complete fusion suppression above the barrier for ^{6,7}Li+^{209}Bi was pointed out in Ref. [13].

Since the calculation of the complete and the incomplete fusion cross section following either the strictly theoretical definitions or the experimental ones is extremely complex, simplifying models have been used up to now [13,15–18]. Using full coupled channel calculations, complete fusion was interpreted in Refs. [16,17] as absorption from projectile bound states, and as incomplete fusion from unbound states. In our approach in Ref. [17], the total fusion cross section for ^{11}Be+^{208}Pb was unambiguously (referred to the strictly theoretical definition) calculated, but this was not the case for the complete and incomplete fusion independently. The unambiguous prediction of complete and incomplete fusion cross sections is still a challenge for all current fusion models [13].

Following Ref. [16], we interpreted in Ref. [17] the total fusion of ^{11}Be on ^{208}Pb as the absorption of the center of mass (c.m.) of the projectile from either its bound or breakup states. Since the mass of the ^{10}Be core is much larger than the neutron mass, such an absorption could ensure that at least the charged core is captured. However, we doubt that this approach can be used to study the total fusion of the two-cluster projectiles ^{6,7}Li because the two charged frag-

*Email address: A.Diaz-Torres@theo.physik.uni-giessen.de

ments (^{6}Li=α+d and ^{7}Li=α+t) have similar masses. In this case, the capture of the c.m. of the projectile is not necessarily connected to the capture of the charged fragments. Therefore, we will use for the present reactions two optical potentials for the nuclear interaction between the projectile fragments and the target. At the same time, the short-ranged imaginary fusion potential defined in the c.m. coordinate of the projectile and used in Ref. [17], will be removed. The imaginary part of those optical potentials will also be short ranged (inside the Coulomb barriers) to ensure that the absorption is associated with fusion channels only.

The present work particularly aims at (i) investigating the relative importance of breakup and bound-state structure effects [i.e., ground-state reorientation couplings, coupling to the bound excited state (^{7}Li) , and bare potential] for the total fusion of ^{6,7}Li on ^{59}Co and ^{209}Bi targets around the Coulomb barrier, (ii) clarifying whether or not the enhancement or suppression effect of breakup is shown in total fusion, and (iii) testing the model with recent experimental data [13,14]. In Sec. II, the theoretical formalism is presented, whereas the results and the discussion are shown in Sec. III. We draw conclusions in Sec. IV.

II. THEORY

Calculations of total fusion cross sections for ^{6,7}Li on ^{59}Co and ^{209}Bi are carried out using a three-body model [17] with a new continuum discretized coupled channel (CDCC) [24] method of calculating fusion, i.e., with short-range fusion potentials for each fragment separately. Full coupled channel calculations are performed with the code FRESCO [25]. The set of coupled equations [17] for the projectile-target radial wave functions is solved with the usual scattering boundary conditions [25].

The total fusion cross section is calculated in terms of that amount of flux which leaves the coupled channels set (total absorption cross section) because of the short-ranged imaginary parts iW_F of the optical potentials between the projectile fragments and the target. This guarantees that at least one of the charged fragments of the projectile is captured. The same Woods-Saxon potential W_F with parameters W_0=−50 MeV, r_0=0.8 fm , and a=0.1 fm is used for the imaginary part of the two optical potentials. The results depend only very weakly on the parameters of this potential, as long as it is well inside the Coulomb barrier and strong enough for the mean free path of the projectile inside the barrier to be much smaller than the dimensions of W_F. The fusion cross sections for W_0=−50 MeV are those for W_0=−10 MeV changed by ~1%. The use of a short-ranged imaginary potential is equivalent to the use of an incoming boundary condition inside the barrier for each fragment to study fusion [26].

In calculations of total fusion cross sections, we simultaneously include (i) the breakup of the projectile caused by inelastic excitations to different partial waves in the continuum (nonresonant and resonant breakup), induced by the projectile fragments-target interactions (Coulomb+nuclear) and (ii) all continuum (bound-continuum and continuum-continuum) and reorientation couplings. By breakup we mean the elastic dissociation of ^{6,7}Li into two fragments only, namely, α+d for ^{6}Li and α+t for ^{7}Li, and not further breakup of the deuteron or triton. The reorientation couplings refer to the couplings of the quadrupole term of the projectile fragment-target potentials, among the projectile-target partial waves, for the projectile in its ground state. Since we will first focus on effect of projectile excitation, we will not include transfer or inelastic channels of the target. The target will be regarded as a spherical nucleus with spin zero. Afterwards, we will estimate the effect of target excitations on the total fusion cross section. We expect both that such an effect could be important at energies just around the Coulomb barrier and that it is similar for the two lithium isotopes.

We would like to stress that in the present calculations the imaginary parts of the off-diagonal couplings have been neglected, while the diagonal couplings include imaginary parts. The reason for not including the imaginary part of the off-diagonal couplings is that they produce numerical instabilities. The Hermiticity of the symmetric breakup matrix is violated when large values of off-diagonal imaginary couplings are included. Those imaginary couplings describe absorption occurring during the transitions between the channels. Following Ref. [27], we expect that these couplings weakly affect the total fusion cross section. In that reference, it was shown that the imaginary off-diagonal coupling redistributes, among the elastic and nonelastic channels, the flux that has already penetrated the Coulomb barrier. The total fusion cross section, however, remained unchanged.

In addition to the Coulomb interaction, the global Woods-Saxon parametrization given in Ref. [28] for the Christensen and Winther potential is used for the real part of the optical potentials between the projectile fragments (^{6}Li=α+d and ^{7}Li=α+t) and the target. Those potentials are given in Table I. The projectile-target bare potential for a central collision is calculated by the single folding of the projectile fragments-target monopole (real) interactions with the ^{6,7}Li ground-state densities defined in terms of the ground-state wave functions. In the following, by Coulomb barrier V_B we mean the barrier of that potential.

The couplings are taken into account up to a projectile-target radial distance $R_{\rm coup}$=150 fm. Partial waves for the projectile-target relative motion up to only $L_{\rm max}\sim 30$ (partial-wave total fusion cross section $\lesssim 10^{-3}$ mb) are included in the calculation.

The bound states of the two-body ^{6}Li(^{7}Li) projectile and the single energy scattering wave functions which form the continuum bins [17] are obtained by solving a Schrödinger equation with the α-d (α-t) potential $V^l_{\alpha\text{-}d}$ ($V^l_{\alpha\text{-}t}$), which may be l dependent. The continuum states with a given partial wave l have been consistently generated either by the same potential as that of the bound state of the same orbital angular momentum l or by the potential generating the unbound resonances. The continuum (nonresonant and resonant) breakup subspace is discretized in equally spaced momentum bins with respect to the momentum $\hbar k$ of the α-d (α-t) relative motion. The bin widths are suitably modified in the presence of the resonant states in order to avoid double counting.

The J^π=1^+ (l=0 coupled to the spin of the deuteron s=1) ground state of ^{6}Li with a binding energy of −1.47 MeV can be generated by a Woods-Saxon potential given in Table I.

TABLE I. Potentials between the projectile fragments and the target are shown along with those to describe the projectile states (g.s.—ground state, res—resonances, b.s.—bound states). The potential depths are given in MeV, and the radii and diffusenesses in fm.

Potential	V_0	r_0	a_0	$V_0^{s.o.}$	$r_0^{s.o.}$	$a_0^{s.o.}$
α-^{59}Co	−31.1368	1.1273	0.63			
α-^{209}Bi	−33.9497	1.1675	0.63			
d-^{59}Co	−19.9336	1.0895	0.63			
d-^{209}Bi	−21.0497	1.1422	0.63			
t-^{59}Co	−25.2677	1.1128	0.63			
t-^{209}Bi	−25.1141	1.1578	0.63			
^{6}Li (g.s.)	−78.46	1.15	0.7			
^{6}Li (res)	−80.0	1.15	0.7	2.5	1.15	0.7
^{7}Li (b.s.)	−108.1	1.15	0.7	0.9875	1.15	0.7
^{7}Li (res)	−109.89	1.15	0.7	1.6122	1.15	0.7

The d-state (l=2,s=1) component [29] of the ground-state (g.s.) wave function has been neglected. The 3^+, 2^+, and 1^+ (l=2 coupled to the spin of the deuteron s=1) unbound resonant states of ^{6}Li can be obtained with a Woods-Saxon potential including a spin-orbit term with the same geometry (see Table I). The energies and widths obtained for those resonances are compared with the experimental [30] values in Table II.

In the case of ^{7}Li, the $3/2^-$ ground state and the bound $1/2^-$ excited state (l=1 coupled to the spin of the triton s =1/2) with binding energies of −2.47 MeV and −1.99 MeV, respectively, can also be reproduced by a Woods-Saxon potential with a spin-orbit term (see Table I). The $7/2^-$ and $5/2^-$ (l=3 coupled to the spin of the triton s =1/2) unbound resonant states are calculated in the same way (see Table I). The energies and widths obtained for those resonances are included in Table II.

For the reactions with ^{6}Li, we obtain converged total fusion cross sections [17] using (i) a maximum energy of the continuum states of 8 MeV for energies well above the Coulomb barrier and of 6 MeV for energies around the barrier, (ii) continuum partial waves up to l=2 waves for a density of the continuum discretization of 2 bins/MeV(l=0,1); 7.7 bins/MeV and 1.92 bins/MeV below and above the 3^+ resonance, respectively, 10 bins/MeV inside the resonance; 2.5 bins/MeV and 2 bins/MeV below and above the 2^+ resonance, respectively, 2.5 bins/MeV inside the resonance; for 1^+ continuum states the density of the discretization is the same as that for 2^+ states, (iii) the projectile fragments-target potential multipoles up to the quadrupole term ($K\leqslant 2$).

For ^{7}Li, converged total fusion cross sections are obtained using (i) the same cutoff for the maximum energy of the continuum states as that for ^{6}Li, (ii) continuum partial waves up to l=3 waves for a density of the continuum discretization of 2 bins/MeV (l=0,1,2); 7.7 bins/MeV and 1.92 bins/MeV below and above the $7/2^-$ resonance, respectively, 10 bins/MeV inside the resonance; 2.5 bins/MeV and 2 bins/MeV below and above the $5/2^-$ resonance, respectively, 2.5 bins/MeV inside the resonance, (iii) the projectile fragments-target potential multipoles up to the octupole term ($K\leqslant 3$).

III. RESULTS AND DISCUSSION

A. ^{6,7}Li+^{59}Co

Figure 1 is used as an example to show the convergence of the total fusion cross sections of ^{6}Li+^{59}Co with respect to the number l of partial waves in the continuum along with potential multipoles K. The maximum energy E_{max} of the continuum states and the density of the continuum discretization are as mentioned above. In particular, we would like to point out that converged results at energies just around the Coulomb barrier are obtained with a small number of continuum partial waves, i.e., up to d waves in the present example, in contrast to what it was claimed in Ref. [21]. In the following, total fusion cross sections refer to converged values.

TABLE II. Energies $E_{\rm res}$ (MeV) and widths $\Gamma_{\rm res}$ (MeV) of the calculated resonances are compared with the experimental values [30].

Projectile	Res	$E_{\rm res}$	$\Gamma_{\rm res}$	$E_{\rm res}^{\rm expt.}$	$\Gamma_{\rm res}^{\rm expt.}$
^{6}Li	3^+	0.73	0.034	0.716	0.024
^{6}Li	2^+	3.09	1.3	2.84	1.7
^{6}Li	1^+	4.67	4.2	4.18	1.5
^{7}Li	$7/2^-$	2.17	0.071	2.16	0.093
^{7}Li	$5/2^-$	4.09	0.6	4.21	0.88

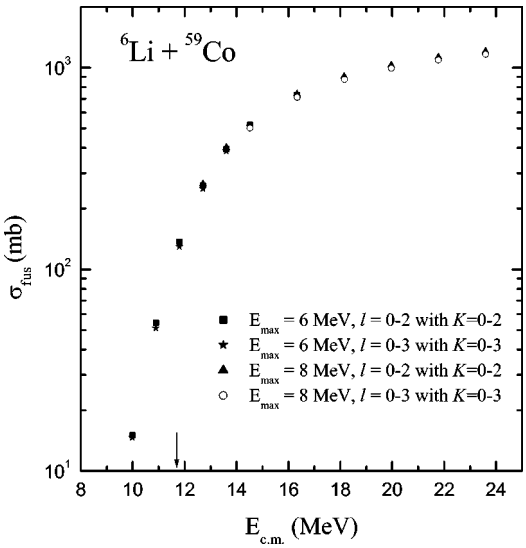

FIG. 1. Convergence of the total fusion cross sections for ^{6}Li $+^{59}$Co with regard to the number l of continuum partial waves along with the potential multipoles K. The arrow indicates the value of the Coulomb barrier. See text for further details.

Figure 2 shows total fusion excitation functions for ^{6}Li $+^{59}$Co (full dots with solid curve) and ^{7}Li$+^{59}$Co (full triangles with dashed curve), which are normalized with the corresponding cross sections in the absence of couplings to breakup channels. For each reaction, the incident energy is normalized with its Coulomb barrier V_B. The Coulomb barrier for ^{6}Li$+^{59}$Co is V_B=11.74 MeV , whereas for ^{7}Li$+^{59}$Co it is V_B=11.68 MeV. These barriers are similar to those (11.5 MeV and 11.35 MeV, respectively) calculated using the double-folding procedure with the Skyrme-type nucleon-nucleon interaction [31]. The total fusion excitation functions

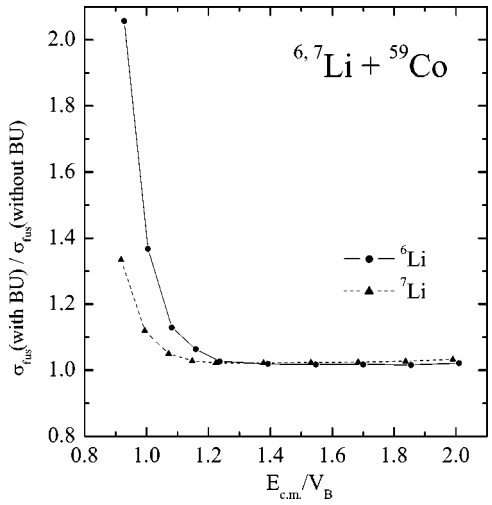

FIG. 2. Total fusion excitation functions for ^{6}Li$+^{59}$Co (full dots) and ^{7}Li$+^{59}$Co (full triangles), which are normalized with the cross sections in the absence of couplings to breakup (BU) channels. For each reaction, the incident energy is normalized with the Coulomb barrier V_B of the bare potential. The calculated values are connected with curves to guide the eye. See text for further details.

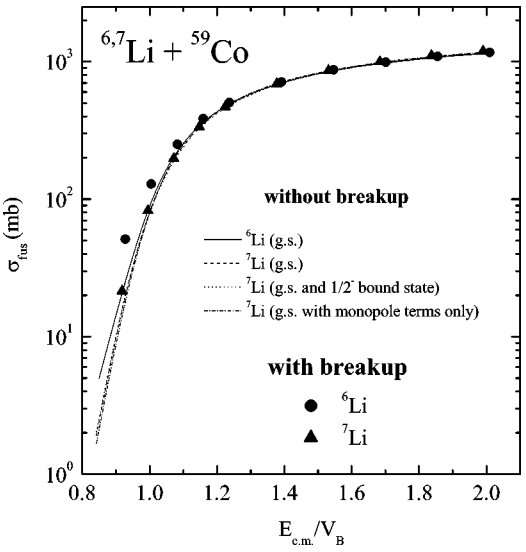

FIG. 3. Total fusion excitation functions for ^{6}Li$+^{59}$Co are compared to those for ^{7}Li$+^{59}$Co. For each reaction, the incident energy is normalized with the Coulomb barrier of the bare potential (fusion without breakup). The reorientation couplings are only included (fusion with breakup). All continuum and reorientation couplings are included. See text for further details.

without breakup include all reorientation couplings of ^{6,7}Li. In case of ^{7}Li, it also includes the coupling to the bound $1/2^-$ first excited state. Since ^{6}Li is a spherical nucleus in its ground state and, therefore, the quadrupole term of the projectile fragments-target potentials is zero, no reorientation effects occur for ^{6}Li. The total fusion excitation functions with breakup include all continuum and reorientation couplings.

The breakup enhances the total fusion cross section at energies just around the barrier, whereas it hardly affects (an enhancement by $\sim$2%) the total fusion at energies well above the barrier. The fusion enhancement around the barrier is larger for ^{6}Li than for ^{7}Li, and it correlates with the smaller α-breakup threshold for ^{6}Li. Here, the enhancement factor strongly depends on the incident energy. This enhancement is caused by the bound-continuum couplings [17] which dominate the suppression effect of the continuum-continuum couplings.

In Fig. 3, we compare the total fusion excitation functions of the two reactions. For each reaction, the incident energy is also normalized with the Coulomb barrier V_B of the bare potential. We only include the reorientation couplings in fusion without breakup. All continuum and reorientation couplings are included in fusion with breakup. We can observe that the total fusion excitation functions without breakup are practically the same for ^{6,7}Li. The mass difference between ^{6,7}Li explains the remaining difference between their fusion excitation functions at energies well below the barrier. Both the ^{7}Li ground-state reorientation effect (comparing the dashed curve to the dash-dotted one) and the effect of the coupling to its bound $1/2^-$ excited state (comparing the dashed curve to the dotted one) on total fusion are very weak.

TABLE III. Experimental values for (i) the first three levels of the ground-state rotational band of the ^{59}Co target [33] and for (ii) the excitations of ^{209}Bi included in the calculation [34].

Target	Energy (MeV)	I^{π}	$B(E\lambda, I \rightarrow \text{g.s.})$ (W.u.)
^{59}Co	0.0	$7/2^-$	
	1.19	$9/2^-$	13.0($E2$)
	1.46	$11/2^-$	5.4($E2$)
^{209}Bi	0.0	$9/2^-$	
	2.493	$3/2^+$	16.0($E3$)
	2.564	$9/2^+$	28.0($E3$)
	2.583	$7/2^+$	25.0($E3$)
	2.599	$11/2^+$	30.0($E3$)
	2.6	$13/2^+$	22.0($E3$)
	2.617	$5/2^+$	22.0($E3$)
	2.741	$15/2^+$	25.0($E3$)

In Fig. 3, we can also observe that the inclusion of the couplings to the breakup channels notably increases the difference between the total fusion excitation functions of the two systems at energies just around the barrier. However, at energies well above the barrier the total fusion cross sections are practically the same. We conclude that the breakup is the main reason for the difference between the total fusion cross sections of ^{6,7}Li on ^{59}Co.

A crude estimation of the effect of ^{59}Co excitations on the total fusion cross section was done by (i) fitting the converged total fusion cross sections of Fig. 3 (with breakup) in a single (elastic) channel calculation by finding an appropriate projectile-target real Woods-Saxon potential with an energy dependent depth and the geometry r_0=1.179 fm and a =0.658 fm, and then (ii) including the target excitations as in Refs. [25,32]. We include the couplings to the first three levels of the ground-state rotational band (Table III) of ^{59}Co [33]. This estimation reveals that the effect is very weak and similar for the two lithium isotopes. Total fusion cross sections are increased by ~5% for energies around the barrier, while they remain constant for energies well above the barrier.

In Fig. 4, the calculated (full squares and triangles) total fusion cross sections of Fig. 3 (with breakup) including the effect of ^{59}Co excitations are compared to the experimental data [14] (open circles and squares). The agreement is good at energies just around the barrier (arrows), but a slight overestimation is observed at energies well above the barrier. However, the ratio of the theoretical cross sections of the two systems agrees very well with the ratio of their experimental cross sections (see Fig. 3 of Ref. [14]) at all energies.

B. ^{6,7}Li + ^{209}Bi

Figure 5 shows, like Fig. 2, total fusion excitation functions for ^{6}Li+^{209}Bi (full dots with solid curve) and ^{7}Li +^{209}Bi (full triangles with dashed curve), which are normalized with the corresponding cross sections without breakup. The incident energies are also normalized with the barrier (V_B=29.71 MeV for ^{6}Li and V_B=29.57 MeV for ^{7}Li) of the calculated bare potentials. These barriers are similar to those

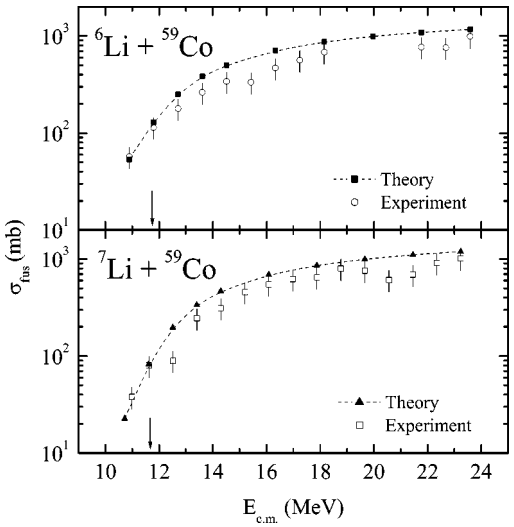

FIG. 4. Calculated (full squares and triangles) total fusion excitation functions for ^{6,7}Li+^{59}Co are compared with the experimental data [14] (open circles and squares). The calculated values are connected with curves to guide the eye. The arrows indicate the Coulomb barriers of the bare potentials. See text for further details.

measured in Ref. [13] (V_B=30.1±0.3 MeV for ^{7}Li and V_B =29.7±0.2 MeV for ^{7}Li) and to those calculated [31] (V_B =29.8 MeV for ^{6}Li and V_B=29.5 MeV for ^{7}Li) with the double-folding procedure.

Fusion enhancement occurs at energies just around the barrier, while breakup has very little effect (an enhancement by ~3.5%) on total fusion at energies well above the barrier. The difference between the two α-breakup thresholds for ^{6,7}Li is also revealed in the value of their enhancement factors around the barrier. These factors also depend strongly on the decreasing incident energy below the barrier. Comparing this figure with Fig. 2, we can observe that the breakup effect on total fusion is stronger for the ^{209}Bi target than for ^{59}Co, as expected.

In Fig. 6, the total fusion excitation functions of the two reactions are compared to each other (as in Fig. 3). It is

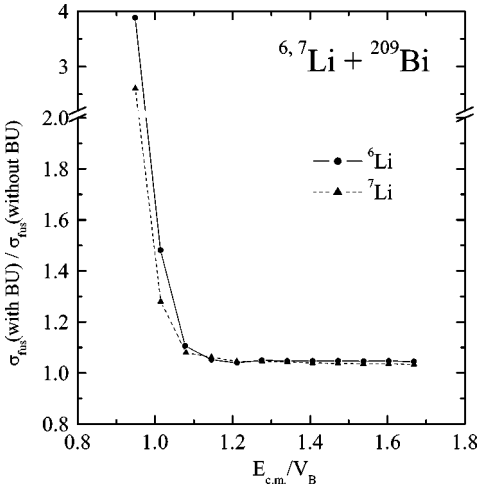

FIG. 5. The same as Fig. 2, but for ^{6}Li+^{209}Bi (full dots) and ^{7}Li+^{209}Bi (full triangles). See text for further details.

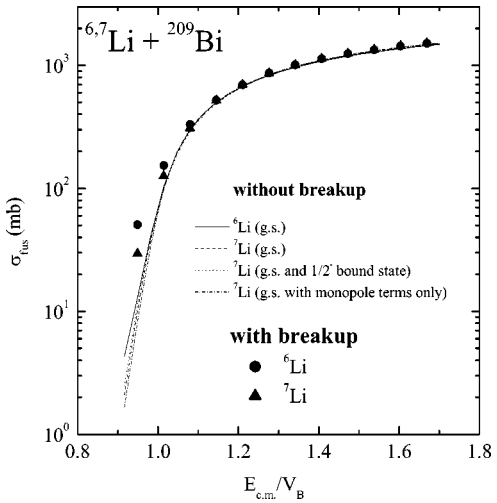

FIG. 6. The same as Fig. 3, but for ^{6,7}Li+^{209}Bi. See text for further details.

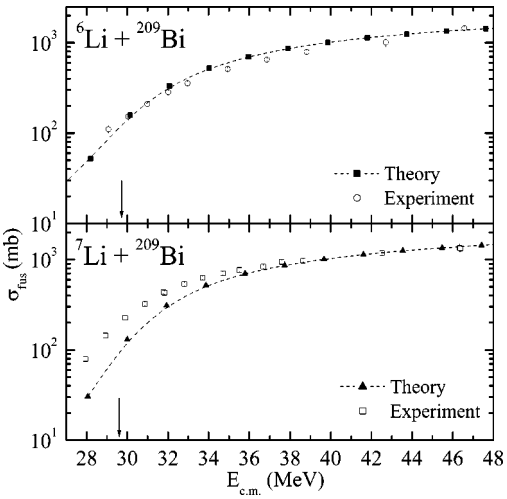

FIG. 7. The same as Fig. 4, but for ^{6,7}Li+^{209}Bi. The experimental data are from Ref. [13]. See text for further details.

observed that the differences between the total fusion excitation functions, caused by the bound-state structure effects of ^{6,7}Li, are very small and similar to those with the ^{59}Co target. The effect of the ^{7}Li ground-state reorientation couplings (comparing the dashed curve to the dash-dotted one) and of the coupling to its bound $1/2^-$ excited state (comparing the dashed curve to the dotted one) on total fusion are also very weak.

In Fig. 6, it is also shown that the breakup increases the difference between the total fusion cross sections for ^{6,7}Li at energies just around the barrier. At energies well above the barrier, the two systems show very similar total fusion excitation functions. Figure 6 also indicates, like Fig. 3, that the breakup causes the difference between the total fusion cross sections of ^{6,7}Li.

We also estimated the effect of target excitations on total fusion. It was done in the same way as for ^{59}Co. Since the couplings to the first two excited states of single-particle structure is rather weak [34], we only include couplings to the collective multiplet $[^{208}\mathrm{Pb}(3^-)\otimes 1h_{9/2}]_{J^\pi}$ (Table III) with energies ranging from 2.493 to 2.741 MeV [34]. Moreover, we assume collective transitions to these excited states due to their complexity (combined collective and single-particle dynamics). Total fusion cross sections remain the same for energies well above the barrier, whereas they are increased by $\sim$3% around the barrier for both ^{6}Li and ^{7}Li.

Figure 7 shows a comparison between the calculated (full squares and triangles) total fusion excitation functions including the effect of target excitations and the experimental data [13] (open circles and squares). The experimental data for ^{6}Li (upper part, open circles) are well reproduced, but it is not the case for ^{7}Li (lower part, open squares). Theoretical results for ^{7}Li underestimate the experimental values at energies around the barrier, but the agreement is good at energies well above the barrier.

In contrast to ^{6,7}Li+^{59}Co [14], experimental total fusion cross sections for ^{7}Li+^{209}Bi are larger than those for ^{6}Li +^{209}Bi around the barrier. The experiment [13] shows that it is because the direct production of ^{210,211}Po evaporation residue (contributing to the incomplete fusion yield) is notably larger with ^{7}Li than with ^{6}Li. These evaporation residues can be produced by the capture of (i) the deuteron or proton (proton capture following dissociation of $d\rightarrow p+n$) for ^{6}Li and of (ii) the triton for ^{7}Li. A stripping breakup process [35] does not seem to explain the larger production of ^{210,211}Po with ^{7}Li, because the triton binding energy in ^{7}Li is larger than the deuteron one in ^{6}Li. It would be interesting to measure deuteron and triton transfer cross sections for these reactions to clarify the reason for the difference of their ^{210,211}Po yields. We would like to stress that couplings to these transfer channels were not included in the present calculations.

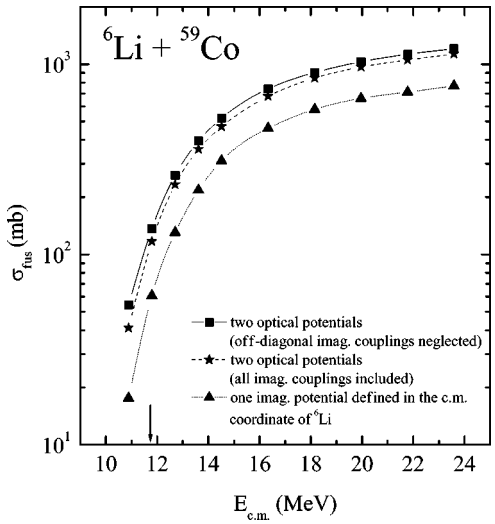

FIG. 8. Total fusion excitation functions for ^{6}Li+^{59}Co using different approaches. The calculated values are connected with curves to guide the eye. The arrow indicates the value of the Coulomb barrier. See text for further details.

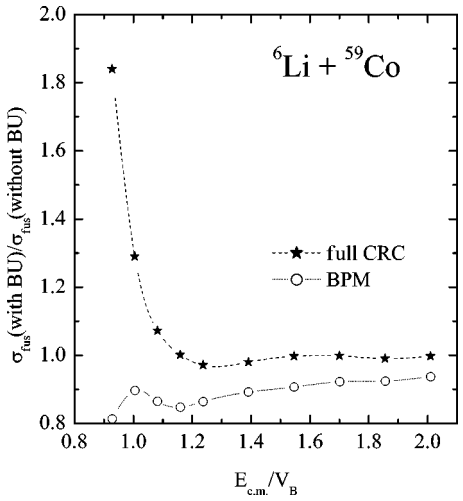

FIG. 9. The same as Figs. 2 and 5, but comparing total fusion excitation functions for ^{6}Li+^{59}Co using two different approaches, namely, full coupled channel calculations (CRC) and the barrier penetration model (BPM). The calculated values are connected with curves to guide the eye. See text for further details.

C. Effect of the off-diagonal imaginary couplings; comparison to other approaches

As an example, Fig. 8 shows the effect of the off-diagonal imaginary couplings on the total fusion of ^{6}Li+^{59}Co. This is the only system (the lightest one studied) for which we have obtained stable results when all imaginary couplings are included, as the off-diagonal imaginary couplings are not too strong in this case. In Fig. 8, we also compare the total fusion excitation function obtained with the present approach (using two optical potentials) to that obtained with our previous method in Ref. [17] (using one imaginary potential defined in the c.m. coordinate of ^{6}Li). The cross sections neglecting the off-diagonal imaginary couplings (full squares in Fig. 8) are the same as shown with full dots in Fig. 3. The cross sections including all imaginary couplings are presented with full stars. The off-diagonal imaginary couplings slightly reduce the total fusion cross sections (by ~13% around the barrier and by ~6% well above the barrier). However, the cross sections obtained with the present approach (full squares) differ considerably from those (full triangles) calculated with the method from Ref. [17], as expected for the ^{6}Li projectile (see Introduction). The results indicate that there are many events where one of the fragments of ^{6}Li is captured, but the c.m. of the projectile does not reach the absorption (fusion) region. The imaginary potential used in the method from Ref. [17] has the same shape and magnitude as the imaginary part of the optical potentials in the present approach.

In Fig. 9, we compare the total fusion excitation function (open circles) obtained with the barrier penetration model (BPM) [27] to that obtained with full coupled channel calculations when all imaginary couplings are included (full stars in Fig. 8). The total fusion excitation functions are normalized with the cross sections in the absence of couplings to breakup channels. The BPM model assumes that all the flux that penetrates a single barrier [defined for these calculations as the sum of the bare potential and the real part of a local dynamic polarization potential (DPP) [32]] leads to fusion. The DPP potential includes the effect of couplings to breakup channels and was extracted from the CDCC calculation shown with full stars in Fig. 8. This approach to fusion has been extensively used in the last few years [19,20] to predict total fusion cross sections with weakly bound projectiles, e.g., very recently for ^{6}Li and ^{6}He on the ^{208}Pb target [20]. It is observed that the BPM cross sections (open circles) underestimate (by ~40% just around the barrier and by ~8% well above the barrier) the actual cross sections (full stars), which is particularly relevant at energies just around the barrier. This is because the BPM approach does not include fusion within the projectile-target barrier [32]. In contrast to the full coupled channel calculations (full stars), the BPM approach (open circles) shows total fusion suppression for the whole range of incident energies studied (by ~14% just around the barrier and by ~9% well above the barrier). The present results shows that the BPM approach is particularly inappropriate at energies just around the barrier and also yields a rather inaccurate answer to the question how breakup affects total fusion.

With the above comparisons, it is important to note that to realistically predict total fusion cross sections the fusion model should be carefully chosen depending on the cluster structure of the weakly bound projectile and on what the experiment is expected to measure (in order to ensure a realistic comparison of theoretical and experimental data).

IV. SUMMARY AND CONCLUSIONS

Total (complete + incomplete) fusion excitation functions of ^{6,7}Li on ^{59}Co and ^{209}Bi targets at Coulomb barrier energies are obtained using full coupled channel calculations with a new CDCC method of calculating fusion, which has short-range fusion potentials for each fragment separately. The realistic prediction of total fusion cross sections requires the selection of an appropriate fusion model which depends on both the cluster structure of the weakly bound projectile and what the experiment is supposed to measure.

The effect of breakup on fusion can be observed in the total fusion excitation function. The breakup enhances the total fusion of ^{6,7}Li at energies just around the barrier, whereas it has very little effect on total fusion at energies well above the barrier. The fusion enhancement factor strongly depends on the decreasing incident energy below the barrier. The fusion enhancement is larger for the reaction with ^{6}Li than that with ^{7}Li, and it is correlated with the smaller α-breakup threshold of ^{6}Li. The difference between the bound-state structures of ^{6,7}Li does not produce large difference between their total fusion excitation functions. The effect of the ^{7}Li ground-state reorientation couplings on total fusion is very weak. A crude estimation reveals that the effect of target excitations on total fusion is weak and similar for ^{6,7}Li. The experimental data for ^{6,7}Li+^{59}Co as well as for ^{6}Li+^{209}Bi are well reproduced. The breakup notably causes the difference between the experimental total fusion cross sections of ^{6,7}Li on ^{59}Co, but it is not the case for the ^{209}Bi

target. Experiments focused on the deuteron and triton transfer cross sections are important to understand the difference between the total fusion of ^{6,7}Li on ^{209}Bi. Work is in progress to study ^{6}He induced fusion reactions since low-energy radioactive beams have become available for new experiments in selected facilities [3,4,7,10].

ACKNOWLEDGMENTS

The authors thank M. Dasgupta for providing experimental data in tabulated form. We would also like to thank G. G. Adamian, N. V. Antonenko, and S. J. Sanders for a careful reading of the manuscript.

[1] A. Yoshida *et al.*, Phys. Lett. B **389**, 457 (1996).
[2] J. Takahashi *et al.*, Phys. Rev. Lett. **78**, 30 (1997).
[3] J. J. Kolata, Eur. Phys. J. A **13**, 117 (2002); J. J. Kolata *et al.*, Phys. Rev. Lett. **81**, 4580 (1998).
[4] K. E. Rehm *et al.*, Phys. Rev. Lett. **81**, 3341 (1998).
[5] M. Dasgupta *et al.*, Phys. Rev. Lett. **82**, 1395 (1999).
[6] E. F. Aguilera *et al.*, Phys. Rev. Lett. **84**, 5058 (2000).
[7] M. Trotta *et al.*, Phys. Rev. Lett. **84**, 2342 (2000).
[8] S. B. Moraes *et al.*, Phys. Rev. C **61**, 064608 (2000).
[9] A. Mukherjee and B. Dasmahapatra, Phys. Rev. C **63**, 017604 (2000).
[10] C. Signorini, Nucl. Phys. **A693**, 190 (2001); C. Signorini *et al.*, Eur. Phys. J. A **5**, 7 (1999); **2**, 227 (1998).
[11] V. Tripathi, A. Navin, K. Mahata, K. Ramachandran, A. Chatterjee, and S. Kailas, Phys. Rev. Lett. **88**, 172701 (2002).
[12] I. Padron *et al.*, Phys. Rev. C **66**, 044608 (2002).
[13] M. Dasgupta *et al.*, Phys. Rev. C **66**, 041602(R) (2002).
[14] C. Beck *et al.*, Phys. Rev. C **67**, 054602 (2003).
[15] L. F. Canto, R. Donangelo, L. M. de Matos, M. S. Hussein, and P. Lotti, Phys. Rev. C **58**, 1107 (1998).
[16] K. Hagino, A. Vitturi, C. H. Dasso, and S. M. Lenzi, Phys. Rev. C **61**, 037602 (2000).
[17] A. Diaz-Torres and I. J. Thompson, Phys. Rev. C **65**, 024606 (2002).
[18] A. Diaz-Torres, I. J. Thompson, and W. Scheid, Nucl. Phys. **A703**, 83 (2002); **533**, 265 (2002).
[19] N. Keeley, K. W. Kemper, and K. Rusek, Phys. Rev. C **65**, 014601 (2002); **66**, 044605 (2002).
[20] K. Rusek, N. Keeley, K. W. Kemper, and R. Raabe, Phys. Rev. C **67**, 041604(R) (2003).
[21] K. Yabana, M. Ueda, and T. Nakatsukasa, nucl-th/0301053.
[22] N. Alamanos, A. Pakou, V. Lapoux, J. L. Sida, and M. Trotta, Phys. Rev. C **65**, 054606 (2002).
[23] D. J. Hinde, M. Dasgupta, B. R. Fulton, C. R. Morton, R. J. Wooliscroft, A. C. Berriman, and K. Hagino, Phys. Rev. Lett. **89**, 272701 (2002).
[24] N. Austern, Y. Iseri, M. Kamimura, M. Kawai, G. Ramitscher, and M. Yahiro, Phys. Rep. **154**, 125 (1987).
[25] I. J. Thompson, Comput. Phys. Rep. **7**, 167 (1988); FRESCO users' manual (version FRXX.09g), University of Surrey, United Kingdom, 2001 (unpublished).
[26] M. J. Rhoades-Brown and P. Braun-Munzinger, Phys. Lett. **136B**, 19 (1984).
[27] G. R. Satchler, M. A. Nagarajan, J. S. Lilley, and I. J. Thompson, Ann. Phys. (N.Y.) **178**, 110 (1987).
[28] R. A. Broglia and A. Winther, in *Heavy-Ion Reactions*, Parts I and II FIP Lecture Notes Series (Addison-Wesley, New York, 1991).
[29] M. V. Zhukov, B. V. Danilin, D. V. Federov, J. M. Bang, I. J. Thompson, and J. S. Vaagen, Phys. Rep. **231**, 151 (1993).
[30] See http://www-nds.iaea.or.at/nudat
[31] N. V. Antonenko (private communication); G. G. Adamian, N. V. Antonenko, R. V. Jolos, S. P . Ivanova, and O. I. Melnikova, Int. J. Mod. Phys. E **5**, 191 (1996).
[32] I. J. Thompson, M. A. Nagarajan, J. S. Lilley, and M. J. Smithson, Nucl. Phys. **A505**, 84 (1989).
[33] M. Baglin, Nucl. Data Sheets **95**, 215 (2002).
[34] M. J. Martin, Nucl. Data Sheets **63**, 723 (1991).
[35] C. Signorini *et al.*, Phys. Rev. C **67**, 044607 (2003).